Dimensioning of partially prestressed concrete beams, optimization of T-shaped section with heels

Sofiane Amziane, Nadim Abdel Nour, Dominique Vié, Alaa Chateauneuf, Assad Kallassy

Dimensioning of Partially Prestressed Concrete Beams, Optimization of T-shaped section with heels

Nadim Abdel Nour[1], Dominique Vié[2], Alaa Chateauneuf[1], Sofiane Amziane[1], Assad Kallassy[3]

[1] University Clermont Auvergne, Institut Pascal, CNRS-UCA-SIGMA, BP 10448, F 63000 Clermont Ferrand, France
[2] Centre des Hautes Etudes de la Construction, 94110 Arcueil, France
[3] Lebanese University, Faculty of Engineering II, Lebanon

Abstract
The present article addresses the structural optimization of partially and fully prestressed concrete bridge girders. For this purpose, an optimization-oriented dimensioning approach for prestressed concrete is proposed in accordance with the Eurocode 2 provisions, it combines all service and ultimate limit states verifications in a coherent manner. An optimization procedure, based on Genetic Algorithms, is conducted on a T-shaped section with heels, with the total cost as the objective function. The design variables are the cross-sectional dimensions, the steel reinforcement and quantity and configuration of prestressing tendons. The constraints include geometrical restraints and verifications under ultimate and service limit states. Numerical examples are implemented to demonstrate the performance and effectiveness of this method, and the results obtained are discussed with final remarks and conclusions.

KEY WORDS: Partial prestressing, Pivot rule, T-shaped heels, Structural optimization, Genetic Algorithms

1 Introduction

Prestressed concrete (PC) has been widely adopted in the design of bridge decks, allowing significant savings in material weight. An engineer's primary goal is to design an optimal structure that satisfies all performance requirements while minimizing the overall cost.

Many optimization techniques have been applied in the design of prestressed concrete bridge decks. Early structural optimization procedures revolved around the simplex method and linear programming, with researchers resorting to simplification techniques to counteract the non-linear constraints. Fereig [1] and Kirsch [2] applied linear programming to the optimal design of prestressed concrete bridge girders, they opted for the linearization of constraints with approximations and certain conditions on the transformation of the design variables to produce linear equations.

Later on, many studies implemented meta-heuristics and evolutionary algorithms in structural optimization (Kaveh [3], Rana [4], Saka [5]), such as genetic algorithms and simulated annealing. These techniques were proved efficient for the resolution of non-linear complex problems such as the design of prestressed concrete bridge decks. Marti [6] successfully applied the simulated annealing algorithm for optimal design of prestressed concrete precast bridges with double U-shaped cross sections. They also presented a cost sensitivity analysis by modifying the steel and concrete unit price. In another study, Yepes and Marti [7] tackle the same subject using four different heuristic algorithms, proving that the best results were obtained using a threshold accepting algorithm. Aydin [8] minimized the cost of prestressed concrete bridge I girders using a genetic algorithm and obtained a solution 28% more economical than the real-life structure.

Given the complexity of the optimization problem involving several design variables and highly non-linear constraints, a suitable optimization-oriented approach for prestressed concrete design is not only effective but also indispensable to facilitate and simplify the optimization procedure, and the exploitation of results, as far as possible.

This paper deals with the structural optimization of partially and fully PC bridge T-shaped girder with heels, manipulating different span lengths. The design strategy developed is outlined at first, and

then the analysis is conducted as a single-objective optimization problem solved using genetic algorithms. Constraints to be satisfied include geometrical constaints and flexural verifications under service and ultimate limit states as per the Eurocode 2 provisions. The entire design and optimization procedure are coded on the computer program "scilab". Numerical examples are presented to demonstrate the efficiency of the developed approach, and the results are analyzed.

The rest of the paper is structured as follows. Section 2 details the methodology developed for both full and partially prestressed sections under service and ultimate limit states. Section 3 is a description of the optimization using Genetic Algorithms. Section 4 defines the optimization problem and states all design variables and constraints. In section 5, a numerical example is presented with parametric studies on several variables (span length, truck live loads, steel ratio ρ and compressive strength f_{ck}) followed by a cost sensitivity analysis and a comparison between the results obtained with fully and partially prestressed sections. Finally, a summary of conclusions is given in section 6.

2 Design strategy

The idea of full prestressing is to maintain the concrete in a compressed state at service loading; the principle of partial prestressing came later on, as an intermediate case between full prestressing and conventional reinforcing, allowing the decompression of concrete and a certain amount of cracking in the service state (Dilger [9], Karayannis [10], Nilson [11], Grebovic [12]).

In the analysis of fully prestressed concrete, the design is based on stress limitations where cracking is not permitted; whereas in partial prestressing, permanent cracks may occur at service loading when the tensile stress exceeds the tensile stress limit of concrete. The concrete section gradually passes from uncracked to cracked state with the increase of loading; cracking is then controlled by limiting the crack width to an allowable value. The crack width limitation can directly be correlated to the tensile steel stress limitation in passive reinforcement. Thus, the main difference between full and partial prestressing is the integration of the crack width limitation in the design which is compensated by the combination of passive and active reinforcement.

The design in partial prestressing is more complicated as it combines full prestressing calculations in the stress analysis and conventional reinforcing calculations in the crack width and tensile stress computation. Design procedures for partial prestressing have not yet been integrated in current codes such as ACI 318 or Eurocode 2, which complexifies the development of a proper design methodology. Partial prestressing procedures proposed by researchers are not included in codes but use considerations from the codes.

Nilson (1976) [11] presented an approach for the calculation of the stresses in partially prestressed beams after cracking. The beam is analyzed as a reinforced concrete member subjected to an eccentric compression force corresponding to the decompression of the concrete.

Dilger and Suri (1987) [9] proposed an approximate formula for the calculation of the tensile steel stress in partially prestressed sections. Values are represented in design charts and can be directly used to determine the maximum crack width. The formula accurately estimates the steel stress for beams with high reinforcement ratio and low degree of prestressing.

Karayannis and Chalioris (2000) [16] developed an approach for predicting the ultimate strength of prestressed concrete beams under pure torsion and torsion combined with shear and flexure. They concluded that the prestressing force can significantly improve the ultimate torsional strength of the section, however this favourable influence decreases as the flexural loads increase. An improvement in the torsion-shear interaction capacity is noticed with the increase of the prestress level.

Rahal (2007) [17] presented a method for the design and capacity calculation of combined torsion and bending strength for reinforced and prestressed concrete sections. The interaction was achieved by superposition of the longitudinal reinforcement in torsion and bending. The analysis was compared to the ACI equations that were found more conservative.

Karayannis and Chalioris (2012) [10] applied partial prestressing on a flexural reinforced concrete beam with rectangular and T-shaped sections. The tensile steel stress is estimated based on the allowable crack width, then the effective pre-strain and prestressing force are calculated.

Turkeli and O zturk (2017) [18] performed optimization of the cost of an I shaped partially prestressed concrete section using Genetic Algorithm. Design variables include cross sectional dimensions and the numbers of active and passive steel reinforcement. Constraints considered are flexural stress, initial camber, dead loads and live loads deflection, ductility, shear strength, ultimate strength and geometrical / reinforcement constraints. The Genetic Algorithm was successfully applied to the section studied by Nilson [11] and a 39% cost reduction was achieved. It was found that the probability to the convergence of the algorithm increases with the population size, however the total calculation time increases leading to a common disadvantage of the Genetic Algorithm.

Lee et al. (2018) [19] proposed a simple method to estimate the net tensile stress of the prestressing steel under service loads according to the ACI 318 provisions. They performed non linear flexural analysis showing that the net tensile stress of cables at service loads increases as the yield strength of cables increase and as partial prestressing decreases. The simplified proposed method was found more conservative than the non linear analysis and can be used as an alternative for the serviceability design.

Many researchers have demonstrated the advantages of partial prestressing over full prestressing. Nilson [11] and Karayannis [10] stated that partially prestressed beams may display a lower upward camber and creep deformation due to the reduced prestressing force. Furthermore, failure of beams with smaller amount of prestress may occur in a ductile manner as opposed to the brittle failure of heavily prestressed beams.

The design theory presented herein, the pivot rule method, is a newly developed approach for dimensioning fully and partially prestressed concrete sections. It draws inspiration from common engineering practice seeking to optimize the design, and it can easily be implemented in optimization algorithms.

The main advantage of this method is the coherent combination of all limit states verifications in one formula along with the formwork condition; it also introduces the prestressing force P as a probable value varying between two limits $\alpha_{min}P \leq P_0 \leq \alpha_{max}P$. The permissible domain of P is found based on a pivot rule, similar to the one used in reinforced concrete, demonstrating the benefit of partial prestressing.

2.1 Conventional design method

The former concrete prestressing French code BPEL prescribed direct limitations on tensile/compressive stresses in extreme fibers of the concrete section under all service limit states. These restrictions were replaced in Eurocode 2 (EC) [13] by limitations on crack width and on stresses in concrete and in active/passive reinforcement depending on the service limit state (quasi-permanent, frequent or characteristic).

Today in common practice, engineers try to avoid the numerous Eurocode verifications by adopting supplementary limitations similar to those specified in BPEL.Each service limit state is characterized by the extreme values of moments and their corresponding stress limitations:

- M_{min} and M_{max}: minimum and maximum values of moment with ΔM being the difference between the two
- σ_{sup} and σ_{inf}: concrete stresses on extreme concrete fibers
- $\overline{\sigma_1}$ and $\overline{\sigma_2}$: stress limits at concrete top fiber under M_{min} and M_{max} respectively
- $\overline{\sigma_3}$ and $\overline{\sigma_4}$: stress limits at concrete bottom fiber under M_{min} and M_{max} respectively

Stress limitations

$$\overline{\sigma_1} \leq \sigma_{sup,\ Mmin} \leq \sigma_{sup,\ Mmax} \leq \overline{\sigma_2}$$
$$\overline{\sigma_4} \leq \sigma_{inf,\ Mmax} \leq \sigma_{inf,\ Mmin} \leq \overline{\sigma_3} \quad (1)$$

Formwork condition

$$\frac{\Delta M\ v}{I} \leq \overline{\sigma_2} - \overline{\sigma_1} \qquad \frac{\Delta M\ v'}{I} \leq \overline{\sigma_3} - \overline{\sigma_4} \quad (2)$$

For each service limit state, two values of P ($P_{critical}$ and $P_{over\text{-}critical}$) are computed with their corresponding eccentricities, and the final prestressing force is the highest value.

2.2 New pivot rule method

This approach considers P to be an external force acting on the concrete section. The crack width limitation is replaced by a limitation on the stress in passive reinforcement by a correlation according to EC.

Stress at section "s" $$\sigma(s) = (1 - \frac{s}{x})\sigma_{sup} \quad (3)$$

Stress at bottom concrete fiber $$\sigma_{inf} = \frac{x - h}{x}\sigma_{sup} \quad (4)$$

Stress at steel location $$\sigma_{st} = \alpha_e \frac{x - d}{x}\sigma_{sup} \quad (5)$$

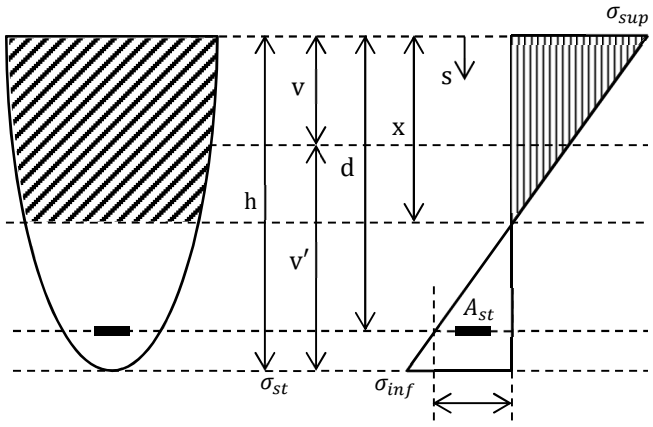

Where :

s position of calculation counted from top

x neutral axis position

σ_{inf} stress at bottom concrete fiber

σ_{sup} stress at top concrete fiber

σ_{st} stress at passive reinforcement A_{st}

α_e equivalence coefficient

Fig. 1 Stress diagram along the height of the concrete section

Mechanical properties of the section with respect to the neutral axis, area A_h, static moment $S_{h/x}$ and moment of inertia $I_{h/x}$:

$$A_h = \int_0^x b(s)\,ds + \alpha_e A_{st} \qquad S_{h/x} = \int_0^x (x - s)b(s)\,ds + \alpha_e A_{st}(x - d)$$
$$I_{h/x} = \int_0^x (x - s)^2 b(s)\,s + \alpha_e A_{st}(x - d)^2 \quad (6)$$

In the case of a T-shaped section with heels where the width is considered linearly variable for each segment, the mechanical properties can be obtained by successive integration using the following equations:

$$\frac{dI_{h/x}}{dx} = 2S_{h/x} \qquad \frac{dS_{h/x}}{dx} = A_h \qquad \frac{dA_h}{dx} = b(x) \quad (7)$$

The equilibrium equations of the bending moment and axial forces, expressed in terms of the mechanical properties of the section, result in the principle equation representing the basis of this approach.

$$P = \frac{\sigma_{sup}\, S_{h/x}}{x} \qquad M^* = Pe_0 + M_{ext} \qquad f(x) = I_{h/x} + \left(\mathrm{v} - x - \frac{M^*}{P}\right) S_{h/x} = 0 \quad (8)$$

The stress limitation is a rupture line represented in the plane (P, M*), prior to the calculation of the cable eccentricity e_o. The neutral axis position is calculated in terms of the prestressed force P by solving the following equation:

$$M^* = P\left[\frac{I_{h/x}}{S_{h/x}} + \mathrm{v} - x\right] \tag{9}$$

At top concrete fiber

$$S_{h/x} = \frac{Px}{\overline{\sigma_{sup}}} \tag{10}$$

At bottom concrete fiber

$$S_{h/x} = (x-h)\frac{P(x-h)}{\overline{\sigma_{inf}}} \tag{11}$$

At passive reinforcement location

$$S_{h/x} = \frac{\alpha_e P(d-x)}{\overline{\sigma_{st}}} \tag{12}$$

The idea is to find the value of the eccentricity e_o for which all service stress limitations are verified for all the applied external moments, taking into consideration the variation of the prestressing force. The actual applied state of stress is represented by a point in the plane (P, M*), and for the section to be verified, that point should be located inside the rupture line for all moment values between M_{min} and M_{max} and all force values between P_{min} and P_{max}.

2.3 Correlation between crack width and stress on steel reinforcement

Following the same annotations as Eurocode 2 [13], the crack width is given by:

$$w_k = S_{r,max}(\varepsilon_{sm} - \varepsilon_{cm}) \tag{13}$$

The difference between the mean strain of the concrete and the steel reveals an effective depth

$$h_{c,eff} = min\{2{,}5(h-d); (h-x)/3\,; h/2\} \tag{14}$$

As long as the neutral axis is located below the top concrete fiber, the limitation of the effective depth to $h/2$ is not controlling, and a value x_0 can be noticed below which the depth is controlled by the first condition.

$$x < x_0 = 7.5d - 6.5h \quad \Rightarrow \quad h_{c,eff} = 2.5\,(h-d) \tag{15}$$

In that case, which is very commonly encountered, it would be equivalent to limit the crack width or the value of the steel stress to the following

$$\overline{\sigma_{st}} = minimum\left\{\frac{5}{3}\frac{E_s w_k}{S_{r,max}}\,;\ \frac{E_s w_k}{S_{r,max}} + \alpha_e K_t f_{ct}\left(1 + \frac{A_{c,eff}}{\alpha_e A_{st}}\right)\right\} \tag{17}$$

In the other case, it would still be possible to determine a position of the neutral axis for which the crack width limitation is reached, while fixing the stress at the top concrete fiber under the maximum moment.

2.4 Fully prestressed/uncracked section

When the section is fully compressed, the mechanical properties are computed in the range [0, h]. Substituting the corresponding expressions of $S_{h/x}$ and $I_{h/x}$ back into equation (8), the position of the neutral axis is found by solving the equation $f(x) = 0$. The well-known stress equations at the extreme concrete fibers for a fully prestressed section are then found.

Permissible domain in full prestressing:

The permissible domain is drawn by expressing the main stress limitations in the plane (P, M*). It is delimited by 4 lines parallel to each other two by two, forming a parallelogram.

Each of the lines corresponds to a stress limitation or pivot, (d1) and (d2) at the top concrete fiber and (d3) and (d4) at the bottom concrete fiber.

At the top concrete fiber: $$(d1): \frac{I_h}{v}\overline{\sigma_1} - \rho v' P \leq M^* \leq \frac{I_h}{v}\overline{\sigma_2} - \rho v' P: (d2) \quad (18)$$

At the bottom concrete fiber: $$(d3): \rho v P - \frac{I_h}{v'}\overline{\sigma_3} \leq M^* \leq \rho v P - \frac{I_h}{v'}\overline{\sigma_4}: (d4) \quad (19)$$

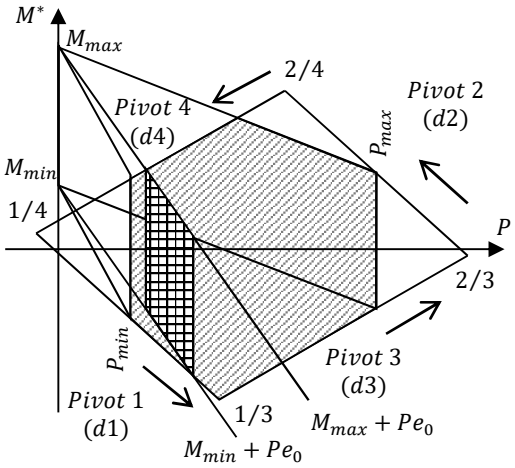

Moving along the contour line of the permissible domain, at each of the lines (d1) to (d4), one stress limitation is reached. At the intersection of two lines, two stress limitations are reached simultaneously. No stress limitation is reached inside the domain.

The known values of P_{min} and P_{max} can be obtained graphically, and are multiplied by the coefficients α_{min} and α_{max} for each limit state.

Fig. 2 Permissible domain in full prestressing

Based on the above detailed principles, a permissible domain can be plotted for any prestressed concrete section. The domain can refer to one service limit state or combine several service limit sates, the same principle applied in both cases.

Pivot 1 denotes the line (d1) that represents the tensile stress limit $\overline{\sigma_1}$ reached at concrete top fiber under M_{min}, pivoting around 1 clockwise goes through all stress states until reaching the tensile stress limit $\overline{\sigma_4}$ at concrete bottom fiber under M_{max} keeping $\overline{\sigma_1}$ at concrete top fiber. Pivoting around 1 in anti-clockwise rotation goes through all stress states until reaching $\overline{\sigma_3}$ compressive stress limit at bottom concrete fiber under M_{min}. This pivot rules applies to all four pivots shown on the domain.

Each boundary line corresponds to a reached stress limit under the applied exterior moments M_{max} or M_{min}. The values of P_{min} and P_{max} can be obtained and represented graphically which will allow the designer to clearly define the range of the permissible values of P, taking into consideration its variation between the coefficients α_{min} and α_{max}. The domain also highlights the P_{max} value that is not usually accorded much importance in conventional design methods but can be controlling at early contruction phases.

The lines M_{ext} + Pe_0 can be very useful to check the variation of the eccentricity with respect to the required prestressing force, the slope e_0 dictates the prestressing condition: critical or over critical section.

The dimensions of a predefined section with any couple (P, e_0) can be graphically verified: the intersection between the vertical line P and (d4) is determined graphically then a line with a e_0 slope is drawn from this point, its intersection with the vertical axis M* represents the capacity of the section and is compared to the applied exterior moment M_{max}. If the obtained moment value is bigger than M_{max} then the section design is adequate.

For a fixed value of the eccentricity e_o, the total moment defined as M* varies in terms of P:

$$M_{min} + Pe_0 \leq M^* \leq M_{max} + Pe_0 \tag{20}$$

The permissible range for the variation of the prestressed force P combining all service limit states:

$$\max(\alpha_{min} P_{min}) \leq P \leq \min(\alpha_{max} P_{max}) \tag{21}$$

2.5 Partially prestressed/cracked section

For an induced tensile stress less than the tensile stress limit, the full prestressing strategy applies. When this limit is exceeded, the section becomes cracked. Partial prestressing includes both passive and active reinforcement in the dimensioning of the section at service and ultimate limit states, whereas passive reinforcement is only used for ultimate verifications in fully prestressed sections.

The same expressions of the force P and the total moment M* can be applied in terms of the neutral axis position. Considering that the section is uncracked under M_{min} (pivots 1 and 3) and cracked under M_{max}, the same value of M^*_{min} is obtained, and M^*_{max} is computed on three different segments.

Pivot 2a = pivot 2, uncracked section

$$M^*_{max} = \frac{I_h}{\mathrm{v}} \overline{\sigma_2} - \rho \mathrm{v}' P \tag{22}$$

Pivot 2b, cracked section

$$M^*_{max} = \overline{\sigma_2} \left[\frac{I_{h/x} + (\mathrm{v} - x) S_{h/x}}{x} \right] \tag{23}$$

Pivot 4b, cracked section

$$M^*_{max} = \frac{\overline{\sigma_{st}}}{\alpha_e} \left[\frac{I_{h/x} + (\mathrm{v} - x) S_{h/x}}{(d - x)} \right] \tag{24}$$

The neutral axis position x_o for which the stress limitations at the upper concrete fiber and the location of the passive reinforcement are simultaneously reached under M_{max} (pivot 2b/4b):

$$x_0 = \frac{\alpha_e \overline{\sigma_2}}{\overline{\sigma_{st}} + \alpha_e \overline{\sigma_2}} d \qquad P_0 = \frac{\overline{\sigma_2} S_{h/x_0}}{x_0} = \frac{\sigma_s S_{h/x_0}}{\alpha_e (d - x_0)} \tag{25}$$

For $P \leq P_o$, pivot 4b is reached; otherwise, pivot 2b is reached.

The same principle as followed in full prestressing still applies for the computation of the forces $P_{critical}$, $P_{over-critical}$ and P_{max}.

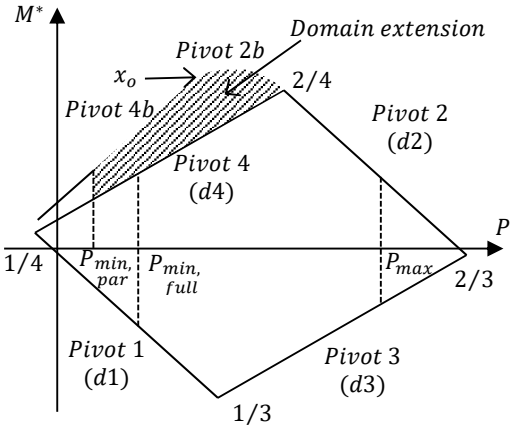

It can be clearly seen that the extended part of the permissible domain in partial prestressing consists of two curves representing the pivots 2b and 4b.

A significant gain in the value of P_{min} can be obtained in partial prestressing since the line (d4) representing pivot 4 is replaced by the curve 4b shifted furher up.

Fig. 3 Extension of the permissible domain in partial prestressing

The above shown permissible domain in partial prestressing is plotted based on the same principles used for the total prestessing with the only difference that an extension represented by the curves 2b and 4b is obtained due to the cracking of the section. In this case, curve 4b represents the state for which the stress limitation at passive reinforcement is reached, whereas curve 2b denotes a reached stress limitation at the top concrete fiber; both limits are reached under M_{max}. This representation allows the designer to approach the partial prestressing in a similar way to what was previously explained in full prestressing regading the values of P_{min}, P_{max} and the permissible range of P values taking into consideration the coefficients α_{min} and α_{max}.

The diagram can be plotted for different ratios of passive reinforcement allowing the designer to follow graphically the variation of the obtained force P with respect to the percentage of reinforcement. For a fixed percentage of reinforcement and known values of (P, e_0), the section design can be verified graphically: the intersection between the vertical line P and curve 4b or 2b is found, then a line with a slope e_0 is drawn from this point, its intersection with the vertical axis M* represents the capacity of the section and is compared to the applied exterior moment M_{max}. If the obtained moment value is bigger than M_{max} then the section design is adequate. This global domain combines the full and partiall prestressing in one diagram, therefore the section design for both partial and full prestressing can be compared using the same diagram.

The values of $P_{critical}$, $P_{over-critical}$ and P_{max} are obtained by resolving a polynomial equation obtained from equation (9) with the following general form:

$$f(x) = I_{h/x} + (\lambda - x)S_{h/x} - ax + b(x - d) = 0 \qquad (26)$$

The values of a, b and λ differ according to each calculated P value and its corresponding activated pivots. For the resolution of such polynomial functions, the use of Muller's method based on Taylor expansion equation has proved to be extremely efficient.

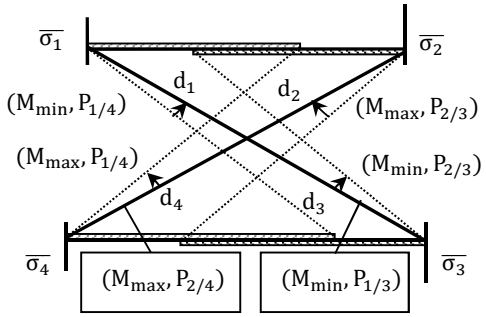

Fig. 4 Pivot rule in full prestressing

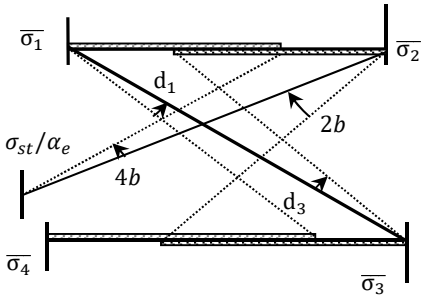

Fig. 5 Pivot rule in partial prestressing

The represented pivot rule should be read in line with the defined permissible domain in both full and partial prestressing. This rule allows the designer to have a better understanding for the prestessed concrete design.

The principle is simple and can be compared to the known pivot rule in reinforced concrete design but with limitation on stresses instead of strains and with linear laws of behavior for the concrete and the steel. For example, pivot 4 represents the state for which the stress limit at the bottom concrete fiber is reached under M_{max}, pivoting around this point is similar to moving along line d4 (defined in the permissible domain), the stress at the top concrete fiber decreases from $\overline{\sigma_2}$ under M_{max} until reaching the limit $\overline{\sigma_1}$ under M_{min} (pivot 1), same pinciple is followed at all pivots allowing the designer to follow the evolution of the stress diagram while moving along the contour of the permissible domain (P, M*).

2.6 Formwork condition

The formwork condition is evaluated, in full prestressing, based on the height of the parallelogram drawn in the plane (ΔM, P). The height shall be sufficient to cover the variations of the exterior moments ($M_{max} - M_{min}$). The same principle applies to partial prestressing; however, a gain in the maximum value of ΔM is obtained based on the new equations of pivots 2b and 4b.

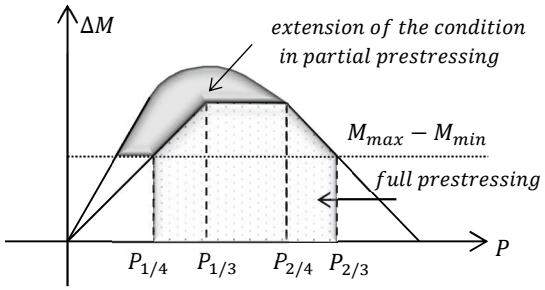

It is worth mentioning that for sections presenting a value of $v/v' < 1$, a gain in the formwork conditions between full and partial prestressing can certainly be obtained.

Fig. 6 Formwork condition in full and partial prestressing

This condition is expressed independently from P and e_o.

2.7 Ultimate bending verification

The verification is based on the interaction diagram, considering the non-linear behavior of the concrete. The points generating the interaction diagram (P, M) correspond to the ultimate states of pivots A, B or C reached, as defined in Eurocode 2.

For the construction of the permissible domain (P, M), the values of the resultants P and M are calculated using the simplified equations below. The section being divided into segments where the width is linearly variable, an integral I_i is introduced and computed for each segment.

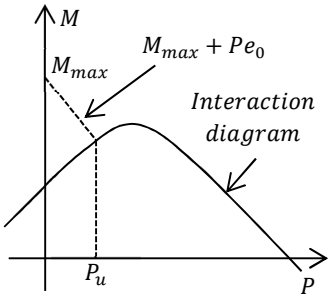

$$N_c(x) = f_{cd}\left\{A_c(x) - \frac{I_n}{(x - x_c)^n}\right\} \quad (27)$$

$$M_{c/C}(x) = f_{cd}\left\{(x_c - x)A_c(x) + S_{c/C}(x) + \frac{I_{n+1}}{(x - x_c)^n}\right\} \quad (28)$$

where x_c is the position for which the strain corresponds to the concrete strain ε_c.

Fig. 7 Interaction diagram in ultimate limit state verification

For a given steel reinforcement ratio, the exact force Pu needed corresponds to the value of P for which the interaction diagram intersects with the line $M_{max} + Pe_o$. The section is verified in the ultimate limit state if the obtained force Pu does not exceed the prestressing force P calculated in the service limit state.

This approach for the ultimate design check is perfectly coherent with the proposed new design method for full and partial prestressing at service limit states. Considering the force P as exterior, this verification is similar to the one used in reinforced concrete but the setion is considered to resist a lower applied exterior moment due to the effect of Pe_0. This means that the prestressing force improves the ultimate capacity of the section by reducing the applied moment.

2.8 Shear verification in service limit state

The provisions of Annex QQ of EC [13] were applied for shear verification in the service limit state. At a distance "d" from the edge of the support, the following interaction equation needs to be verified:

$$\frac{\sigma_1}{f_{ctk,0.05}} + \frac{0.8\,\sigma_3}{f_{ck}} < 1 \qquad (29)$$

where σ_1 and σ_3 are the principal stresses acting on the section, and f_{ck} and $f_{ctk,0.05}$ are the compressive strength at 28 days and the direct tensile strength of concrete respectively.

The computation of the principal stresses σ_1 and σ_3 is based on the normal and tangential induced stresses due to the applied loading on the section. The tangential stresses are directly proportional to the shear force Vu; therefore, taking into account the vertical component of the prestressing force $Psin(\alpha)$, where α is cable angle, reduces the applied shear force. The prestressing force improves then the capacity of the section under shear.

3 Optimization with a genetic algorithm

A genetic algorithm (GA) is an evolutionary optimization method inspired by Charles Darwin's theory of natural selection. The algorithm is based on the concept of "survival of the fittest"; it basically simulates the process of human evolution where the individuals that are most responsive to change are able to survive. This is most known as adaptation; "a biological process, whereby organisms evolve by rearranging genetic material to survive in environments confronting them" as clearly stated by Holland [14].

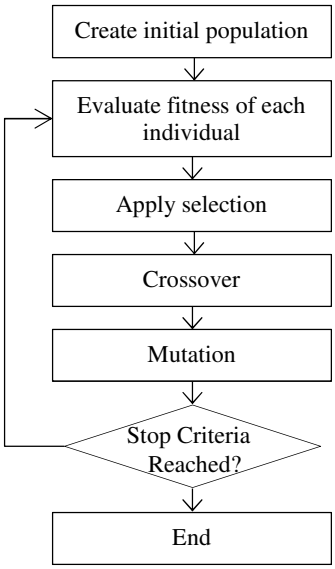

The concept: an initial population of candidates is randomly generated, and then evaluated using a "fitness function" also called an "objective function"; this represents the first generation of solutions. The individuals are categorized according to their fitness, and the genetic operators of selection, crossover and mutation are applied to the population, with different weights, in order to produce an improved next generation better than the previous one. This process is repeated iteratively until the generated individuals converge towards a unique solution, with a pre-fixed convergence rate.

In this study, the initial population is bidimensional and composed of couples (h, b_w) randomly genereated by the algorithm. The user inputs upper and lower bounds of the design variables to be respected by the GA, along with the material properties, loads, combination factors, concrete cover and stress limitations. The population size is taken 100 and the number of generations is 50, these values can be easily modified in the GA program if the user wishes to modify them.

The stop criterion is reached when the solution converges towards a unique value or when the maximum number of generations is reached. This is translated by comparing the absolute difference between the maximum and minimum values of the objective function at each iteration to a fixed threshold value; the GA stops when the difference is less than the threshold. In this work, a value of 10^{-6} is considered for the threshold.

3.1 Genetic operators

GA operators play an important role in the convergence of the mathematical model toward an optimal solution. Operators can be applied with different probability rates depending on the population size and the optimization problem.

3.1.1 Selection

The main idea of selection is to choose the best individuals to undergo crossover and mutation to produce the next generation. Each individual is given a probability of having a descendant proportional to its performance/fitness. Its aim, then, is to favour the most efficient individuals to reproduce more often. The selection operator is applied as many times as necessary to complete the new population.

Many selection procedures have been proposed, including roulette-wheel selection, rank selection and elitism selection [15]. The most suitable selection operator is chosen according to each specific problem in order to increase the optimality of the expected solution.

The default selection procedure adopted for this study is the elitism. The best individuals are selected from the current generation and kept unaltered for reproduction in the next generation. This method guarantees the quality improvement of the solutions iteratively. The selection procedure can certainly be modified in the program to another method.

3.1.2 Crossover

Crossover is a transformation operator that creates a new individual by combining two or more selected parents. The purpose of crossover is to increase the diversity of the population by manipulating the structure of the parent individuals. Its fundamental role is the recombination of the information present in the genetic heritage of the population. It is applied after the selection operator with a fixed probability rate Pc, usually around 0.6. The most popular crossover methods are single-point crossover, multi-point crossover, and uniform crossover.

The crossover function used in the program is an extension of a convexe combination. The crossed individuals are computed from the parent individuals using the following equations:

$$prob = (1 + 2\beta) \times random - \beta$$

$$Crossed\ individual\ 1 = prob \times individual\ 1 + (1 - prob) \times individual\ 2$$

$$Crossed\ individual\ 2 = prob \times individual\ 2 + (1 - prob) \times individual\ 1$$

The parameter β is a positive value; in this case, it is taken as 0 and the resulting crossover is a simple convexe combination. Indidividuals 1 and 2 are the parents and crossed individuals are the resulting descendants after crossover operation.

3.1.3 Mutation

The mutation operator is usually applied after crossover. It modifies an individual randomly and locally to produce new offspring. Since it is a divergence operator, it is applied with a low probability Pm, usually around 0.1. High mutation rate increases the search probability and prevents the population from converging. The role of mutation is to prevent the algorithm from becoming stuck at a local optimum, and avoid premature convergence.

A continuous variable mutation function is used in this study, with a mutation probability of 0.1.

The random mutation operator changes the parent individual bound between fixed upper and lower limits to a mutated individual using the following equation

$$Mutated\ individual = \delta(lower\ bound; upper\ bound)$$

The operator δ denotes the uniform distribution on the interval [lower bound; upper bound] applied with a probability of Pm=0.1. Thus, the mutated individual is independent from the parent individuals.

3.2 Penalty function

Since GAs are mainly used to solve unconstrained optimization problems, the objective function is then expressed as unconstrainted. A penalty function is added to the objective function and used to account for violated constraints; by doing so, the constrained problem is transformed into an unconstrained one. The penalty function is the absolute sum of the normalized violated constraints:

$$p = \sum_{i=1}^{n} p_i \qquad \begin{matrix} p_i = g_i & for\ g_i > 0 \\ p_i = 0 & for\ g_i \leq 0 \end{matrix} \tag{30}$$

where n is the total number of constraints, p_i is the violation factor of the ith constraint, and g_i is the constraint i.

At each evaluation of the objective function, the values of p_i are calculated and the objective function is multiplied by $(1+p)^2$.

For instance, for the verification of the prestressing force P between the minimum and maximum values P_{min} and P_{max}, two penalties are calculated.

The constraints $P \geq P_{min}$ and $P \leq P_{max}$ are translated into the following penalties:

$$p_{Pmin} = absolute\left(\min\left(0;\ 1 - \frac{P_{min}}{P}\right)\right) \qquad p_{Pmax} = absolute\left(\min\left(0;\ 1 - \frac{P}{P_{max}}\right)\right)$$

This means that when the constraint is violated

$$P \leq P_{min} \qquad 1 - \frac{P_{min}}{P} \leq 0 \qquad p_{Pmin} > 0$$

However, when the constraint is satisfied

$$P \geq P_{min} \qquad 1 - \frac{P_{min}}{P} \geq 0 \qquad p_{Pmin} = 0$$

The aim of the penalty function is to increase the value of the objective function when the constraint is violated so that, when evaluating the minimum cost, it is not chosen as an optimal solution.

4 Optimal design of a prestressed concrete beam

4.1 Optimization methodology using scilab

The algorithm is coded on the computer program “scilab”; fully prestressed and partially prestressed sections are coded on two separate programs. All input parameters are provided in an Excel spreadsheet read by the program, and each constraint is introduced as a “scilab function” along with the objective cost function. The procedure is as follows.

The GA generates random populations of the design variables h and b_w respecting the upper and lower bounds provided as input. The initial population size is set to 100 and the number of generations to 50. The genetic operators of selection, crossover and mutation are defined in the program with the corresponding probabilities: elitism selection, crossover with a rate of Pc=0.6 and continuous variable mutation with a rate of Pm=0.1.

For each iteration, or generation, and for each couple [h, b_w] of the initial population, the defined “Cost function” representing the objective function calls another function “Heel Size” for the computation of the heel dimensions of the section.

“Heel Size” contains the calculations of the required prestressing force, number of cables, quantity of passive steel reinforcement and all possible configurations of the prestressing cables and the passive reinforcement that lead to specific dimensions of the heel width and height. For each number of cables, different configurations of cables and passive reinforcement are introduced into the program leading to different heel dimensions. The passive steel reinforcement is initially input; and the configurations that have same number of cables as the obtained value and a passive steel reinforcement ratio equals to or higher than the initially input value are retained. The real prestressing force is

re-calculated for each configuration since the eccentricity differs depending on the tendons and passive steel arrangement.

Based on these results, another function goes through all retained configurations and chooses the heel dimensions and the passive and active steel configuration with the lowest cost; the latter solution is returned to the objective "Cost function". Cost of the heel dimensions includes passive steel, prestressing cables, concrete volume and formwork.

Having chosen the heel dimensions, the cross-sectional dimensions are now all known for a specific couple of [h, b_w]. The constraints are then verified and the ratios of the flexural constraints are calculated to be implemented in the penalty function. The ratio of a constraint is defined as the maximum applied value of the parameter considered over the allowable value.

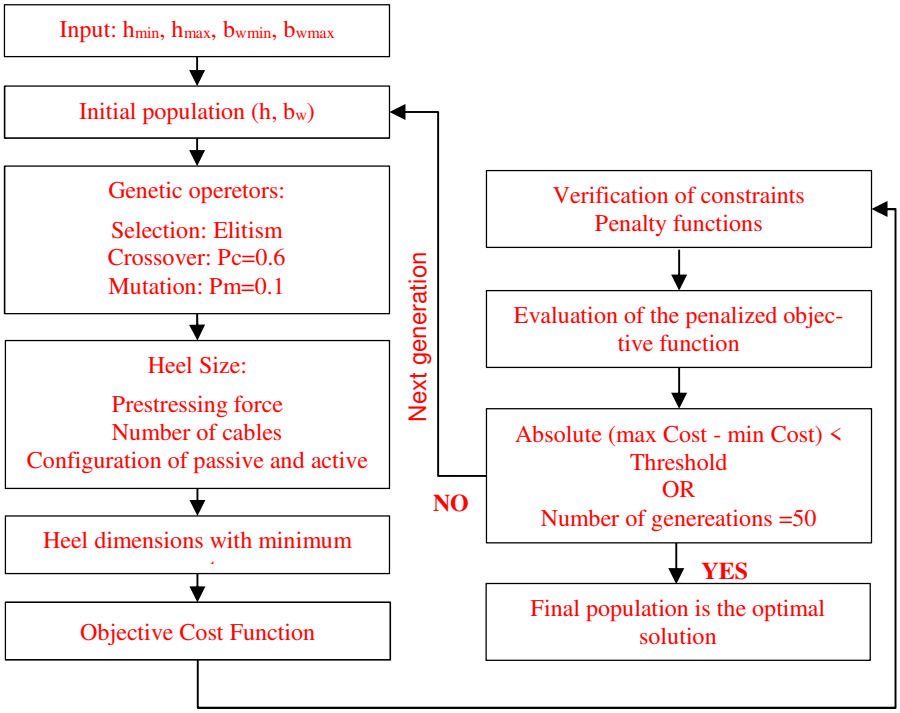

Finally, the penalized objective function is evaluated for each couple of the initial population, and the stop criterion is checked by comparing the difference between the maximum and minimum values of the objective function to the prefixed threshold. If the threshold is not met, then a new population is generated and the GA continues with the same procedure until the stop criteria is met, convergence of the objective function with a 100% rate, or the maximum number of iterations (50 generations) is reached. When the convergence is reached, the final population obtained contains necessarily the same couple (h, b_w) for the entire population.

This program is applicable for partial and full prestressing; different functions for the calculation of the prestressing force and the passive steel reinforcement are used in each case.

4.2 Formulation of the optimization problem

The optimization problem is formulated as:

Minimize $F(x)$	$F(x)$	= objective function
	$g_i(x)$	= set of constraints
Subject to $g_i(x) \leq 0$	x	$= \{x_k\}$ design variables $k = 1, 2, \dots, n$
$x^l \leq x \leq x^u$	x^l	$= \{x_k{}^l\}$ lower bounds of design variables $k = 1, 2, \dots, n$
	x^u	$= \{x_k{}^u\}$ upper bounds of design variables $k = 1, 2, \dots, n$

4.3 Objective function

In this paper, the objective is to minimize the cost of the prestressed concrete beam; this includes the cost of the concrete volume, steel reinforcement, prestressing steel and formwork. The cost is calculated per linear meter of the beam. The objective function is mathematically expressed as

$$F = V_c\, C_c + W_s\, C_s + W_p\, C_p + P_{er}\, C_f \tag{31}$$

Penalized objective function

$$\phi = F\,(1+p)^2 \tag{32}$$

where C_c, C_s, C_p and C_f are the respective unit costs of concrete, steel reinforcement, prestressing steel and formwork. V_c, W_s, W_p and P_{er} are the concrete volume, the weight of steel reinforcement, the weight of prestressing steel and the perimeter of the section respectively.

4.4 Design variables

Table 1 Design variables

Variable	Description	Variable type
h	height of the beam	continuous
b_w	web width of the beam	continuous
b_t	heel width of the beam	continuous
h_t	heel height of the beam	continuous
h_g	bottom sloped height	continuous
n_{As}	number of steel reinforcement	discrete
con	configuration of prestressing tendons	discrete

The design variables include the heel dimensions since this part of the section is responsible for the placement of the tendons and the passive reinforcement with a minimum addition of concrete volume. For the dimensioning of the heel, a data table including all possible tendon configurations for 1 to 10 tendons and passive steel reinforcement is included in the program (see Figure 9).

Passive reinforcement is placed at a location lower than the tendons, closer to the bottom concrete fiber. The number and configuration of steel tendons is computed so as to ensure a maximum steel reinforcement ratio of 1% with a maximum of 2 bundled layers.

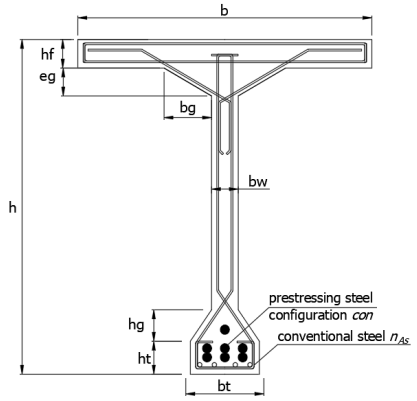

Fig. 8 Typical cross-section of the beam

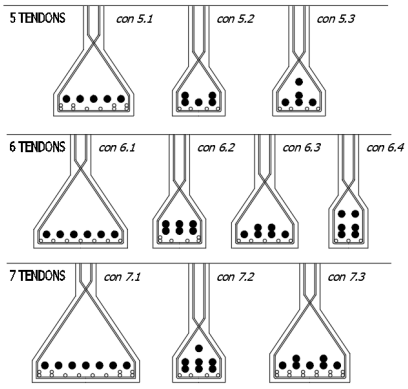

Fig. 9 Tendon configurations example

4.5 Design parameters

The design parameters are constant and therefore are not subject to optimization. They include the loading considered, material properties, unit cost of materials, the slab thickness and the geometrical dimensions not considered as design variables such as the beam top flange width, the top flange thickness, and the top inclination width and depth.

4.6 Constraints

The constraints considered are consistent with the Eurocode 2 provisions, along with geometrical constraints. Flexural constraints are defined as ratios between the applied solicitation (stress, shear, axial force) and the limit calculated using the proposed approach.

Table 2 Constraints

Geometrical constraints	Depth of beam section	$h_{min} \leq h \leq h_{max}$
	Width of web	$b_{w,min} \leq b_w \leq b_{w,max}$
	Width of heel	$b_w \leq b_t$
	Width of web to fit one tendon	$b_w \geq 3\varphi$
Flexural constraints	Minimum prestressing force	$g_1 = 1 - P_{min}/P$
	Maximum prestressing force	$g_2 = 1 - P/P_{max}$
	Formwork condition	$g_3 = 1 - ratio_{formwork}$
	Ultimate bending check	$g_4 = 1 - P_u/P$
	Shear verification	$g_5 = 1 - ratio_{shear}$

φ is the duct size. The beam web width should be sufficient to fit at least one tendon, with clear spacing between tendons equal to the duct size.

5 Numerical example

The structural optimization procedure presented above was applied to a prestressed concrete 3-lane road bridge with a 10m-wide deck composed of three T-shaped girders with heels. The study was computed on the edge beam, which carries the most severe loading following a transverse distribution of the induced loads as per Courbon's method.

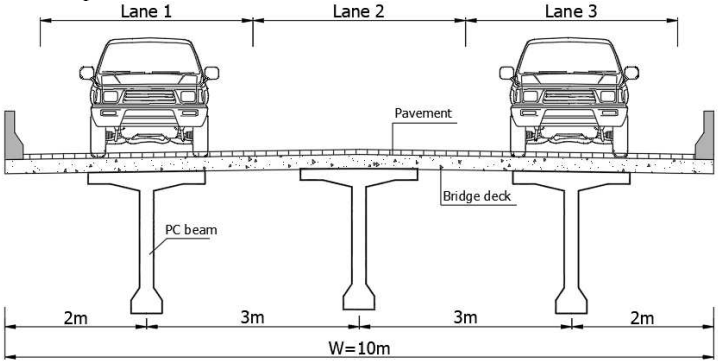

Fig. 10 Cross section of the studied bridge

Table 3 Analysis input parameters and assumptions

Geometric parameters		Loading assumptions	
Beam top flange width	$b = 2m$	Traffic model	LM1
Beam top flange thickness	$h_f = 0.16m$	Concrete unit weight	$25\ kN/m^3$
Top inclination width	$b_g = 0.2m$	Dead loads	$22.5\ kN/m$
Top inclination thickness	$e_g = 0.1m$	Distributed live load	$17.15\ kN/m$
Deck slab thickness	$th = 0.25m$	Truck loads	$544\ kN$
Material properties		**Unit cost of materials**	
Compressive strength	$f_{ck} = 40MPa$	Concrete volume cost	$C_c = €250/m^3$
Tensile strength of passive reinforcement	$f_{yd} = 435MPa$	Steel reinforcement cost	$C_s = €1.2/kg$
Tensile strength of prestressing steel	$f_{pk} = 1860MPa$	Prestressing steel cost	$C_p = €3.6/kg$
Tendon type	$12T15$	Formwork cost	$C_f = €125/m$
Optimization assumptions			
Beam height bound	$1 \leq h \leq 4m$	Population size	100
Web thickness bound	$0.1 \leq b_w \leq 0.4m$	Crossover rate	$P_c = 0.6$
Number of iterations	50	Mutation rate	$P_m = 0.1$

5.1 Parametric study and discussion of results in full prestressing

A parametric study has been carried for different span lengths, to test the influence of the following 3 parameters on the optimal solution:

- Formwork condition
- Heel dimensions
- Compressive strength f_{ck}
- Ultimate bending check
- Truck live loads
- Steel reinforcement ratio

5.1.1 Formwork condition of the optimal solution

The formwork condition is the controlling verification in the service limit state; it is very interesting to study its variation for different span length and different loading assumptions such as the TS variation considered here. This condition is represented by the ratio between the applied moment variation $\Delta M = M_{max} - M_{min}$ and the maximum allowed moment variation ΔM_{max}.

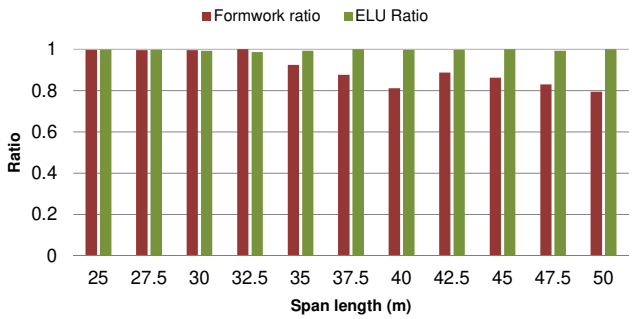

Fig. 11 Variation of the formwork condition with span length for TS=544KN

The results show that for spans of less than 40m, the formwork condition is dominant and has a great influence on the optimal solution, as its value nearly reaches 1. The same applies for the ultimate ratio ELU. For longer spans, the formwork ratio plays a less important role in the search for the optimal solution, whereas the ELU ratio remains controlling.

5.1.2 Heel dimensions of the optimal solution

The heel of the section plays an important role in the optimization procedure and significantly affects the optimal solution obtained, since it increases the total concrete and formwork cost. Its dimensions should be determined with the sole purpose of placing the required tendons and steel reinforcement obtained in the design. In order to evaluate its influence on the section dimensions, the area of the heel is calculated for all obtained optimal sections having different numbers of prestressing tendons.

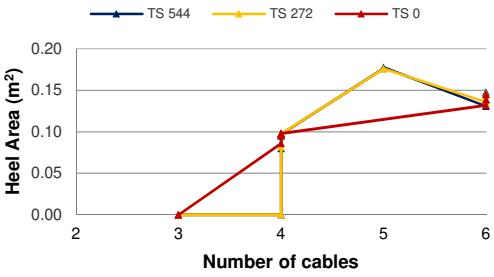

Span Length (m)	Cable number	Heel area (m^2)
25	3	0
30	4	0.0798
35	4	0.0970
40	5	0.1776
45	6	0.1390
50	6	0.1478

Fig. 12 Heel area as a function of number of cables Table 4 Results for $TS = 544kN$

As can be seen, the heel area is null where the number of cables is less than or equal to 4, which means that the section becomes a simple Tee section; and it increases as the number of cables rises. The heel is then clearly dimensioned in the optimization algorithm to fit the tendons and the steel reinforcement without adding value to the design capacity of the section.

5.1.3 Influence of shear force on the optimal solution

The web width is normally controlled by the applied shear force. In order to study the influence of the shear on the web width, the optimization procedure is repeated with different truck live loads TS, normally taken as $TS = 544kN$ in the LM1 model. For each span between 20m and 50m in a 5m increments, and for each TS value ($0kN$, $272kN$ and $544kN$), two ratios are calculated:

- ratio_V representing the capacity of the section to resist the shear force, meaning if the ratio_V is equal to 1 then the section has reached its maximum shearing capacity
- ratio $3\varphi/b_w$, a geometric ratio between the minimum web width needed to allow the profiling of the cables and the optimal web width

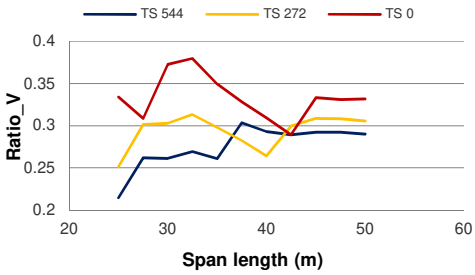

Fig. 13 Effect of TS on ratio_V

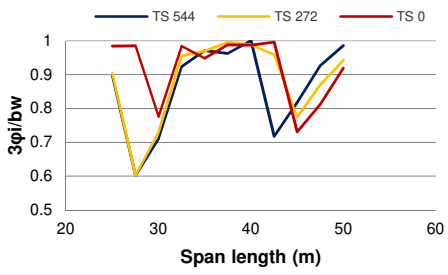

Fig. 14 Effect of TS on ratio $3\varphi/b_w$

The graphs plotted in Figures 13 and 14 show that Ratio_V remains around 0.3 for all spans and TS values, whereas ratio $3\varphi/b_W$ is saturated at spans between 30m and 40m, and close to 1 in other cases as well.

The results demonstrate that the web width is not controlled by the shear force but rather by the geometric criterion of allowing the change in tendon elevations through the section.

5.1.4 Influence of the applied live loads on the slenderness ratio

The slenderness ratio is directly related to the ratio M_{min}/M_{max} of the applied loads. Higher values of the moment ratio mean higher slenderness. For the purpose of this study, different values of truck loads TS were taken, and the corresponding slenderness ratio were computed for each of the obtained optimal solutions, for spans between 25m and 50m.

Slenderness ratios exceeding 22 can be reached for moment ratios around 0.7 at characteristic load combination.

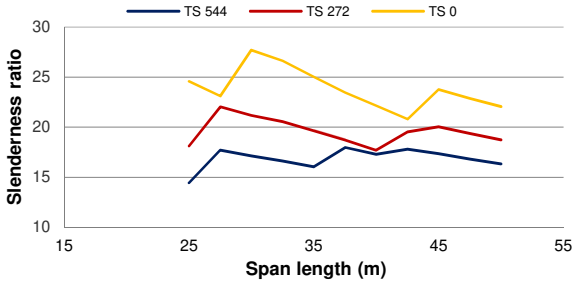

Fig. 15 Effect of the applied loads on the slenderness ratio

5.1.5 Influence of the compressive strength on the optimal solution

The influence of the compressive strength f_{ck} on the optimal solution is examined by applying different values ranging from 30MPa to 60MPa, in increments of 10MPa for span length of 30m, 40m and 50m for fully prestressed sections.

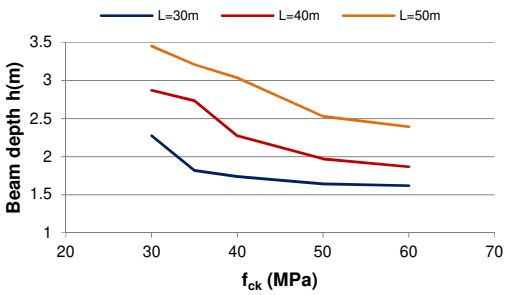

Fig. 16 Effect of f_{ck} on the beam height

f_{ck} (MPa)	h (m)	Slenderness
30	2.87	13.93
40	2.27	17.60
50	1.97	20.29
60	1.87	21.41

Total reduction of 34.9%

Table 5 Results for 40m span length

It can be seen that by increasing the compressive strength of concrete, the total depth of the section is decreased. A reduction of 35% is noted when f_{ck} increases from $30MPa$ to $60MPa$ for a span length of 40m. An interesting parameter in bridge cost analysis is the slenderness ratio (span / height), which is highly influential when evaluating the feasibility of the project in the preliminary phase. Increasing the concrete compressive strength leads to an increase in the slenderness ratio proportional to the decrease of the beam depth.

The ratios of formwork condition and ultimate limit state of the optimal solution remain the same and are unaffected by the variation of the compressive strength.

5.1.6 Steel reinforcement ratio parametric study

In fully prestressed sections, the passive steel reinforcement values are usually added for verification of the section in the ultimate limit state. As a first step, the dimensions of the section are determined in the service limit state with a minimum ratio of steel reinforcement; nonetheless, as can be seen in Figure 11, the ELU ratio is saturated for spans less than 40m, and determines the section for spans greater than 40m. This has led to an analysis of the influence of the reinforcement ratio on the optimal solution in fully prestressed sections.

The results show a gradual decrease in the optimal beam depth with increasing steel reinforcement ratio, leading to a rise in the slenderness ratio. This is accompanied by an increase in the prestressing force P, the number of cables and the heel area. The increase in heel area is due to the necessity to install more steel reinforcement, whereas the increase in the prestressing force is due to a lower value of the cable eccentricity induced by the addition of steel reinforcement, since the cables are placed above the passive reinforcement. It should be noted that if a reduction in the beam depth is not sought, the optimal solution in full prestressing is obtained for a minimal amount of steel reinforcement.

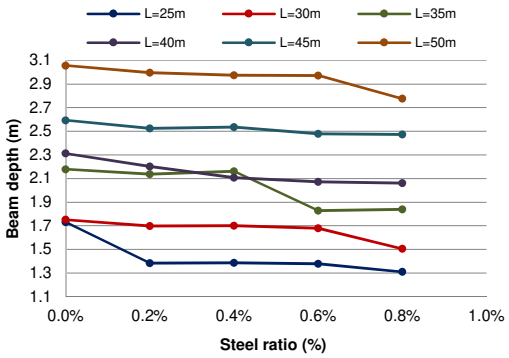

Fig. 17 Effect of steel ratio on the beam height

Span	h_0%	h_0.8%	Reduction
25m	1.730	1.310	24.27%
30m	1.752	1.505	14.08%
35m	2.179	1.838	15.64%
40m	2.313	2.061	10.90%
45m	2.593	2.474	4.61%
50m	3.057	2.776	9.21%

Table 6 Beam height reduction for steel ratios of 0% and 0.8%

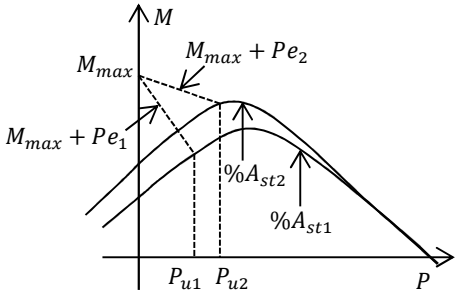

Fig. 18 Interaction diagram for two different steel ratios

On another level, for a fixed beam height, an increase in the steel ratio would normally improve the ultimate capacity of the section. However, this can be seen on condition that the eccentricity of the cable remains unmodified, since the ultimate moment to be verified is the sum of the applied moment and the moment caused by the axial prestressing force $M_{ELU} + P\, e_0$.

5.2 Cost sensitivity analysis

The sensitivity to unit costs of the concrete and the prestressing steel is investigated in order to test their impact on the design. The concrete unit cost is increased from 0 to $€350/m^3$ in increments of $€50/m^3$, meaning the variation ranges between 0.4 C_c and 1.4 C_c; and the impacts on the concrete area and beam depth are studied. The prestressing unit cost is also increased from 0 to $€5.76/kg$ in increments of $€0.72/kg$, with the variation then ranging between 0.4 C_p and 1.6 C_p; and the impact of the number of cables and the beam height are investigated. The formwork cost is taken as 0 in both cases.

As expected, the results indicate that the concrete unit cost has a major impact on the total area of the section and the beam depth. At lower concrete unit costs, the beam depth and area are at their highest values, and they start to decrease as the concrete cost rises. A sudden decrease in beam height and the area is depicted at a different unit cost for each span length, as shown in Figures 19 and 20. This means that it would be more economic, for a higher unit concrete cost, to have a section with a reduced area and an increased number of cables.

As for the prestressing steel unit cost variation, for lower values, the number of cables is at its highest and the beam depth at its lowest; then the beam depth and the total concrete section start to increase with increasing unit prestressing cost, reaching a value very close to the maximum allowed by the user h_{max}, whereas the number of cables normally decreases. The overall trends shown in these graphs are logical and make perfect sense.

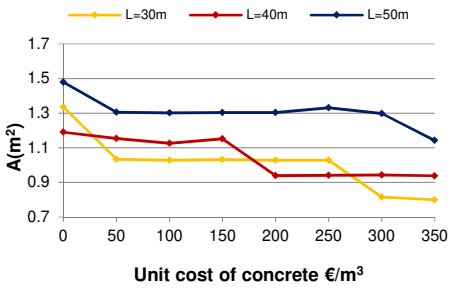

Fig. 19 Effect of the concrete cost on the area

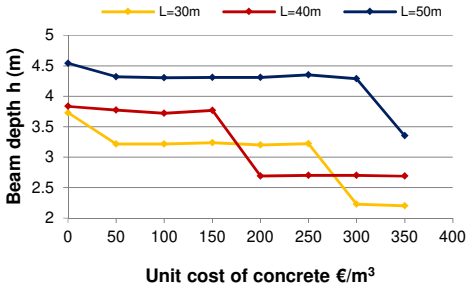

Fig. 20 Effect of the concrete cost on the depth

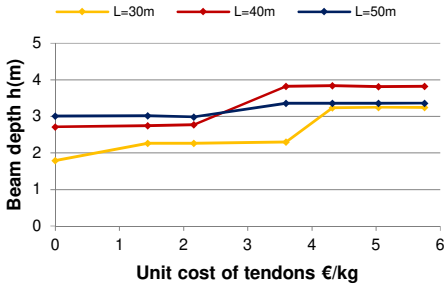

Fig. 21 Effect of the tendons cost on the depth

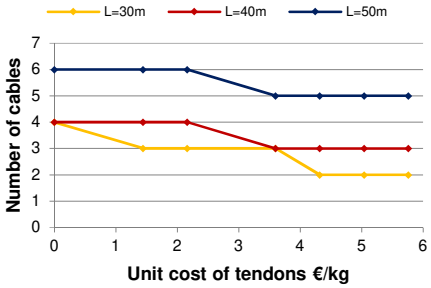

Fig. 22 Effect of the tendon cost on the cables

Table 7 Variation of concrete unit cost for a span of 40m

C_c	$h(m)$	$A(m^2)$	$cables$
0	3.834	1.190	3
0.4 C_c	3.718	1.126	3
0.6 C_c	3.768	1.152	3
0.8 C_c	2.692	0.939	4
1.0 C_c	2.699	0.941	4
1.2 C_c	2.699	0.942	4
1.4 C_c	2.688	0.938	4

Table 8 Variation of tendon unit cost for a span of 40m

C_p	$h(m)$	$A(m^2)$	$cables$
0	2.712	1.040	4
0.4 C_p	2.746	1.006	4
0.6 C_p	2.772	1.204	4
0.8 C_p	3.819	1.204	3
1.0 C_p	3.838	1.204	3
1.2 C_p	3.816	1.204	3
1.4 C_p	3.820	1.204	3

If the formwork cost is taken into consideration, Figures 23 and 24 below show that the beam depth is slightly affected by the variation of both unit costs of concrete and prestressing steel, the trends in both graphs are roughly constant.

In summary, unit costs are of great importance, and majorly affect the optimal solution. Their values should be thoroughly and carefully chosen, and they can vary with time and from country to country.

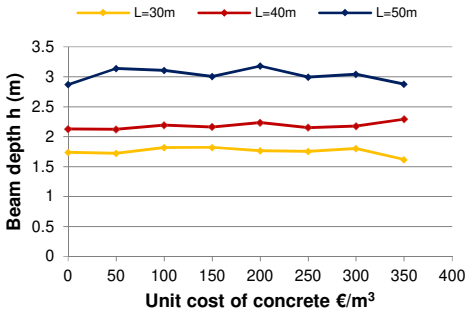

Fig. 23 Effect of concrete cost on the area

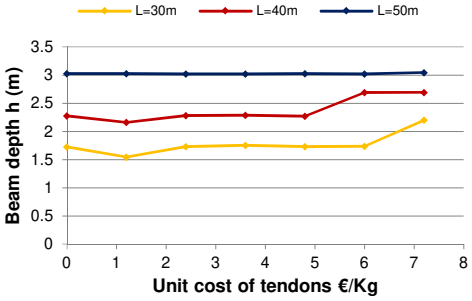

Fig. 24 Effect of concrete cost on the depth

5.3 Discussions on partial prestressing optimization

5.3.1 Influence of the compressive strength on the optimal solution

Compressive strength f_{ck} varied between $30MPa$ and $60MPa$ in increments of $10MPa$ for a span of $40m$ and steel reinforcement ratios of 0.6% and 0.8%.

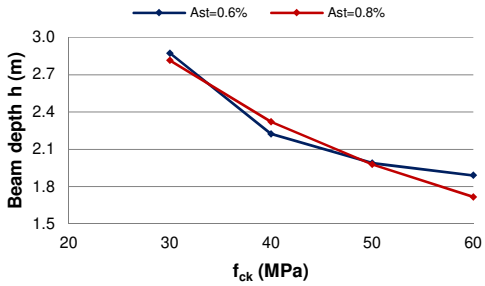

Fig. 25 Effect of f_{ck} on the beam depth

f_{ck}(MPa)	30	40	50	60
h (m)	2.87	2.22	1.98	1.89
A_h (m2)	1.10	0.96	0.90	0.87
P (MN)	7.71	10.91	11.16	10.97
$cables$	3	5	5	5

Table 9 Variation of f_{ck} for 0.6% steel ratio

The variation of the compressive strength has the same effect in partially prestressed sections as in fully prestressed ones. An increase in f_{ck} from $30MPa$ to $60MPa$ leads to a decrease of the beam height of 39% for a steel ratio of 0.8% and a span length of 40m. However, this decrease is attended by a logical increase in the prestressing force and the number of cables.

Similar to the fully prestressed sections results, the formwork and ultimate ratios are unaffected by the change of the compressive strength.

5.3.2 Influence of the steel ratio on the optimal solution

The steel reinforcement ratio plays an important role in partial prestressing design as it contributes to the service capacity of the section, and therefore to its dimensioning. The optimization procedure is conducted for different steel reinforcement ratios ranging between 0.2% and 0.8% with an increment of 0.2%, and for span lengths between $25m$ and $50m$ with a of $5m$ increment.

The results show a decrease in the prestressing force of the optimal solution with increasing steel reinforcement ratio, along with a slight decrease in beam height. The drop in the prestressing force is not as significant as that found in the partial prestressing design theory, with the extension of the permissible domain, since the values are computed for the optimal section at each steel ratio, meaning that the geometric dimensions of the sections including the heel change with the steel ratio.

The formwork condition graph Figure 28 shows a significant decrease with the increase in the steel ratio, whereas the ultimate constraint (ratio ELU) remains saturated for all steel ratios, (Figure 29). Hence, the optimal solution is controlled by the ultimate condition, as was the case with full prestressing.

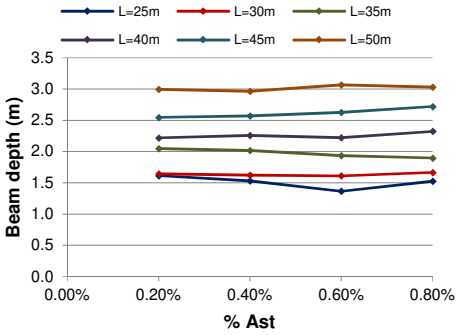

Fig. 26 Effect of % A_{st} on beam depth

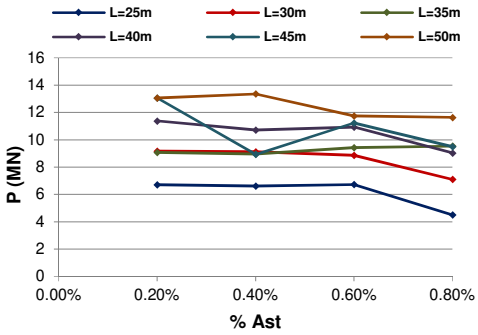

Fig. 27 Effect of % A_{st} on prestressing force

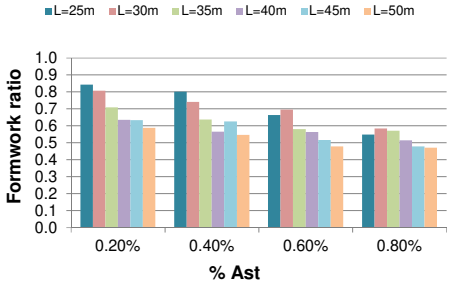

Fig. 28 Effect of % A_{st} on formwork ratio

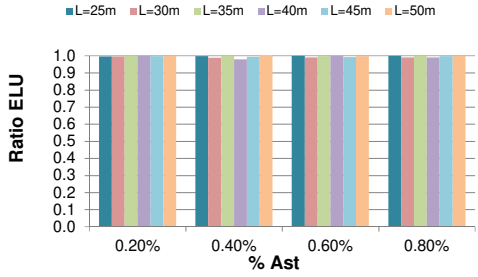

Fig. 29 Effect of % A_{st} on ultimate ratio

In order to clearly show the effect of the extension of the permissible domain and the decrease of P in partial prestressing, the same section dimensions were retained and different steel ratios are applied.

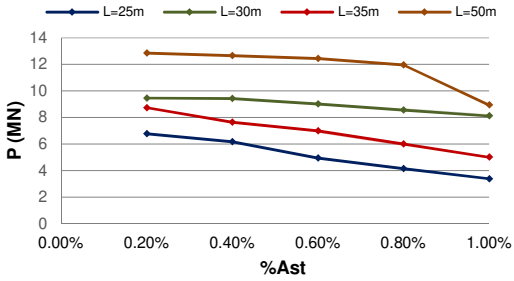

The decrease in the prestressing force is significant and reached a reduction of 50% when the steel ratio increases from 0.2% to 1.0%, for a span length of $25m$ and a 42% reduction for a span length of $35m$.

Fig. 30 Effect of % A_{st} on prestressing force

5.4 Comparative analysis between full and partial prestressing

Table 10 Results for the optimal solution in full and partial prestressing

Span length (m)	L=25m				L=40m			
Steel ratio (%)	0.40%		0.60%		0.60%		0.80%	
Prestressing	Full	Partial	Full	Partial	Full	Partial	Full	Partial
P (MN)	10.45	6.61	10.39	6.73	14.95	10.92	15.10	9.04
Cables number	4	3	4	3	6	5	6	4
Formwork ratio	1.00	0.80	1.00	0.66	0.77	0.56	0.75	0.51
Area (m^2)	0.82	0.66	0.80	0.73	1.02	0.97	1.04	0.99
Cost (€)	1019.66	959.43	1021.95	993.48	1398.90	1382.97	1412.16	1375.45

The results show a significant decrease in the prestressing force, the number of cables and the formwork condition in partial prestressing. With a span of $25m$, the prestressing force is reduced by 35% for a steel ratio of 0.4% when considering the section as partially prestressed, and the formwork ratio decreases by 33%. The total area and overall cost of the section decrease in partial prestressing with a less significant rate, while the total cost of the section undergoes a slight decrease.

6 Conclusion

In this paper, the structural optimization of partially and fully PC bridge T-shaped girder with heels is addressed as a single-objective optimization problem solved using genetic algorithms coded on the computer program "scilab". For this purpose, an optimization-oriented dimensioning approach for prestressed concrete is set forth in accordance with the Eurocode 2 provisions, introducing a new pivot rule, similar to the one used in reinforced concrete, but based on the stress limitations instead of the strains. The permissible domain of the prestressing force P and the bending moment M^* is represented demonstrating the benefit of partial prestressing in extending this domain and significantly decreasing P for the same section dimensions.

The following conclusions can be drawn based on the numerical example.

For fully prestressed sections:

- Where the span length is less than $40m$, the optimal solution activates both formwork and ultimate constraints, whereas for larger spans, the ultimate state requires a larger concrete section, which leads to a non-saturated formwork condition.
- The heel of the section is dimensioned to fit the prestressing tendons and the passive steel reinforcement; it has no added value in relation to the section design. When the cables can fit in the web, the heel area is then null.
- A variation in the applied live loads shows that the web width is not controlled by the shear force but rather by the geometric criterion of allowing the cable profile to elevate through the section. On the other hand, the slenderness ratio is greatly affected by the values of the applied loads, ratios exceeding 22 can be obtained for moment ratios M_{min}/M_{max} around 0.7.
- The parametric study of the compressive strength f_{ck} indicates that a reduction of 35% in the beam height, and consequently a 35% increase in the slenderness ratio, can be seen when f_{ck} increases from $30MPa$ to $60\ MPa$ for a span length of 40m.
- Passive reinforcement is used for ultimate verification of the section in full prestressing. A gradual decrease in beam depth is noticed with the increase of the steel reinforcement ratio, accompanied by a rise in the prestressing force P and the heel area. The optimal solution in full prestressing is obtained for the lowest steel ratio in case a reduction in the beam depth is not sought.

- For the same beam depth, an increase in the steel ratio increases the ultimate section capacity, provided the eccentricity of the tendons remains unmodified. The eccentricity of the cables has a significant effect on the ultimate verification.
- A cost sensitivity analysis is conducted showing a great impact of the unit costs of concrete and prestressing steel on the optimal solution. Considering a formwork unit cost of zero, the beam depth and the concrete section decrease with the increase of the unit concrete cost, consequently the number of cables increases to compensate for the reduction in concrete. On the other hand, an increase in the unit cost of prestressing steel leads to a decrease in the number of cables and an increase in the concrete section. If the formwork cost is taken into consideration, the results show that the beam depth is slightly affected by the variation of both unit costs of concrete and prestressing steel.

For partially prestressed sections:

- The variation of the compressive strength has the same effect in partially prestressed sections as in fully prestressed ones. An increase in f_{ck} from $30MPa$ to $60MPa$ leads to a decrease of the beam height of 39% for a steel ratio of 0.8% and a span length of 40m followed by an increase in the prestressing force and the number of cables.
- The prestressing force of the optimal solution decreases with increasing steel reinforcement ratio, along with a slight decrease in beam height. For the same geometric dimensions, the decrease in the prestressing force reaches a reduction of 50% for an increase of the steel ratio from 0.2% to 1.0%, with a span length of $25m$
- The formwork condition ratio significantly decreases with the increase in the steel ratio.
- The ultimate constraint (ratio ELU) remains controlling for all span lengths and steel ratios

Drawing a comparison between full and partial prestressing, the latter allows for a significant reduction in the prestressing force, the number of cables and the formwork ratio with a slight decrease in the total concrete section and the overall cost.

7 Notation list of used variables

P	Prestressing force	f_{cd}	Design compressive strength of concrete
P_o	Probable value of P	w_k	Crack width
$\alpha_{min}, \alpha_{max}$	Lower and upper limits for P factors	ρ	Section efficiency $\frac{I}{A\ v\ v'}$
$M_{min,}\ M_{max}$	Minimum and maximum values of applied moment	I_h	Homogenized moment of inertia of the section
ΔM	$\Delta M = M_{max} - M_{min}$	h	Section height
$\sigma_{sup}, \sigma_{inf}$	Stress at top and bottom concrete fiber respectively	b_w	Web width of the beam
$\sigma_{sup,\ Mmax}$	Concrete stress at top fiber under maximum moment	A_h	Homogenized area of the section
$\sigma_{sup,\ Mmin}$	Concrete stress at top fiber under minimum moment	$I_{h/x}$	Homogenized moment of inertia with respect to the neutral axis
$\sigma_{inf,\ Mmax}$	Concrete stress at bottom fiber under maximum moment	$S_{h/x}$	Homogenized static moment of with respect to the neutral axis
$\sigma_{inf,\ Mmin}$	Concrete stress at bottom fiber under minimum moment	$b(x)$	Width of the section at position x counted from top
$\overline{\sigma_1}$ $\overline{\sigma_2}$	Stress limit at concrete top fiber under M_{min} and M_{max} respectively	e_o	Cable eccentricity counted from the center of gravity
$\overline{\sigma_3}$ $\overline{\sigma_4}$	Stress limit at concrete bottom fiber under M_{min} and M_{max} respectively	P_{min}, P_{max}	Minimum and maximum values of P
σ_{st}	Stress at passive steel reinforcement	$A_c(x)$	Area of the uncracked concrete section

$\overline{\sigma_{st}}$	Stress limitation at passive steel reinforcement	p	Penalty function
I	Moment of inertia of the section	g_i	Constraint number i
v	Distance from the center of gravity to the top fiber	φ	Diameter of prestressing cable sheath
v'	Distance from the center of gravity to the bottom fiber	x	Neutral axis position
α_e	Equivalence coefficient E_s/E_c	s	Position of stress calculation counted from top fiber
Vc, Ws, Wp, Per	Concrete volume, weight of steel reinforcement, weight of prestressing steel and perimeter of the section respectively	d	Distance from the steel reinforcement to the top fiber
Cc, Cs, Cp, Cf	Unit costs of concrete, steel reinforcement, prestressing steel and formwork respectively		

References

[1] S. M. Fereig. 1994. "An Application of Linear Programming to Bridge Design with Standard Prestressed Girders ". *Computers & Structures*, vol. 50, no. 4, pp. 455-469

[2] U. Kirsch. 1972. "Optimum Design of Prestressed Beams". *Computers & Structures*, vol. 2, pp. 573-583

[3] A. Kaveh, M. Maniat, M. Arab Naeini. 2016. "Cost Optimum Design of Post-Tensioned Concrete Bridges Using a Modified Colliding Bodies Optimization Algoritm". *Advances in Engineering Software* 98 (2016) 12-22

[4] S. Rana, N. Islam, R. Ahsan, S. N. Ghani. 2013. "Application of Evolutionary Operation to the Minimum Cost Design of Continuous Prestressed Concrete Bridge Structure". *Engineering Structures* 46 (2013) 38-48

[5] M.P. Saka, O. Hasancebi, Z.W. Geem. 2016. "Metaheuristics in Structural Optimization and Discussions on Harmony Search Algorithm". *Swarm and Evolutionary Computation* 28 (2016) 88-97

[6] J. Marti, F. Vidoza, V. Yepes and J. Alcala. 2012. "Design of Prestressed Concrete Precast Road Bridges with Hybrid Simulated Annealing". *Engineering Structures* 48 (2013) 342–352

[7] V. Yepes, J. V. Marti, T. Garcia-Segura. 2017. "Heuristics in Optimal Detailed Design of Precast Road Bridges". *Archives of Civil and Mechanical Engineering* 17 (2017) 738-749

[8] Z. Aydn and Y. Ayvaz. 2009. "Optimum Topology and Shape Design of Prestressed Concrete Bridge Girders Using a Genetic Algorithm". *Struc Multidisc Optim*, no. 41, pp. 151-162

[9] Dilger W.H. and K.M. Suri. 1986. "Steel Stresses in Partially Prestressed Concrete Members". *PCI Journal*, vol. 31, n° 3, 1986, p. 88-112

[10] C.G. Karayannis and C.E. Chalioris. 2013. "Design of Partially Prestressed Beams Based on the Cracking Control Provisions". *Engineering Structures*, 48 (2013) 402-416

[11] A.H. Nilson. 1977. "Flexural Stresses after Cracking in Partially Prestressed Beams". *PCI Journal* vol. 21, n° 4, 1977, p. 72-81

[12] R. Sindjic-Grebovic. 2012. "Stresses in Prestressing Steel of Partially Prestressed Element with Cracks". *INDIS,* Serbia

[13] Eurocode 2, EN 1992-2:200, Annex QQ 5 and EN 1992-1-1 section 7.3

[14] J. Holland. 1992. *Adaptation in Natural and Artificial Systems.* MIT Press

[15] Edmund K. Burke, Graham Kendall. 2005. *Search Methodologies Introductory-Tutorials in Optimization and Decision Support Techniques*. New York: Springer

[16] C.G. Karayannis and C.E. Chalioris. 2000."Strength of Prestressed Concrete Beams in Torsion". *Structural Engineering and Mechanics*, Vol. 10, No. 2 (2000) 165-180

[17] K. N. Rahal. 2007."Combined Torsion and Bending in Reinforced and Prestressed Concrete Beams Using Simplified Method for Combined Stress-Resultants". *ACI Structural Journal*, Title no. 104-S38

[18] E. Turkeli and H. T. O zturk. 2017. "Optimum Design of Partially Prestressed Concrete Beams Using Genetic Algorithms". *Structural Engineering and Mechanics,* Vol. 64, No. 5, 579-589

[19] D.H. Lee, SJ. Han, HE Joo and K.S. Kim. 2018. "Control of Tensile Stress in Prestressed Concrete Members under Service Loads". *International Journal of Concrete Structures and Materials 12*, Article No. 38